View metadata, citation and similar papers at core.ac.uk

brought to you by CORE

provided by Elsevier - Publisher Connector

Available online at www.sciencedirect.com

ScienceDirect

Procedia CIRP 31 (2015) 287 – 292

www.elsevier.com/locate/procedia

15th CIRP Conference on Modelling of Machining Operations

An analytical model of residual stress for flank milling of Ti-6Al-4V

Xinda Huang[a], Xiaoming Zhang[a,]*, Han Ding[a]

[a]*State key Laboratory of Digital Manufacturing Equipment and Technology, School of Mechanical Science and Engineering, Huazhong University of Science and Technology, Wuhan, 430074, China*

* Corresponding author. Tel.:+86-27-87559842; fax: +86-27-87559416. *E-mail address:* cheungxm@hust.edu.cn

Abstract

Residual stress is one of the most critical parameters in surface integrity, which has a great impact on fatigue life of the machined components. While the flank milling of titanium alloy Ti-6Al-4V has been widely applied to the manufacture of jet engine for its high productivity in aerospace industry, prediction of residual stress induced by this process is seldom reported. In this paper, an analytical model of residual stress is proposed, based on comprehensive analysis of the mechanical loading during flank milling. For the first time, the sequential discontinuous variable loading feature of flank milling is taken into consideration. An incremental elasto-plastic method followed by a relaxation procedure is used to get the stress-strain history of an arbitrary point in the subsurface so as to predict the residual stress retained in the workpiece after several loading cycles. We find that during the last phase in which the machined surface is generated, the main load comes from the plough effect of cutting edge as the uncut depth approaches zero. The simulation results indicate that the flank milled surface shows more compressive residual stress in the axial direction than in the feed direction. To validate the prediction, a series of cutting tests are conducted on Ti-6Al-4V using finish parameters and X-ray diffraction is utilized to obtain the residual stress.

© 2015 The Authors. Published by Elsevier B.V. This is an open access article under the CC BY-NC-ND license (http://creativecommons.org/licenses/by-nc-nd/4.0/).

Peer-review under responsibility of the International Scientific Committee of the "15th Conference on Modelling of Machining Operations

Keywords: Flank milling; Residual stress; Analytical model; Titanium alloy

1. Introduction

Titanium alloys are widely used in aerospace industry for the manufacturing of structure part, gas turbine and compressor impeller etc. As one of typical difficult-to-cut materials, the removal rate of titanium alloy is limited, especially in the finish machining of workpiece with free sculpture surface, where ball end milling is widely used. In order to improve productivity, flank milling is proposed and has been applied to the finish machining of impellor with ruled surface. While most of the researches on flank milling are about the geometrical errors and tool trajectory optimization in the multi-axis flank milling of free-form surface [1], the influence of flank milling on surface integrity, especially the residual stress, of the machined surface is seldom reported.

When it comes to the machining of titanium alloys in the aerospace industry, the residual stress achieved by the final machining process is of considerable importance due to its impact on the fatigue performance of the workpiece. A large number of experimental researches have been carried out in this field, which has been reviewed in detail [2, 3]. The diversity of experimental results is found in the literature due to the comprehensive effects of process conditions. Although the influence of machine process on residual stress can be investigated thoroughly using the FEM-based methods, the huge computation time consumption makes it difficult to apply them to industrial process. As a result, efficient physical based models for the prediction of residual stress in the machined surface are desperately needed.

Several analytical models for residual stress in machining have been proposed. The early work of Liu et al. [4, 5] illustrated the mechanism of residual stress in machined surface by a semi-infinite model for one-dimension elastic-plastic loading, which explained the influence of shear plane, flank wear and cutting parameters. Jacobus et al. [6] proposed a plane-strain thermo-elastic-plastic model for orthogonal machining and accurately predicted the biaxial residual stress profiles beneath the newly machined surface after calibration.

2212-8271 © 2015 The Authors. Published by Elsevier B.V. This is an open access article under the CC BY-NC-ND license (http://creativecommons.org/licenses/by-nc-nd/4.0/).

Peer-review under responsibility of the International Scientific Committee of the "15th Conference on Modelling of Machining Operations
doi:10.1016/j.procir.2015.03.061

Liang et al. [7] proposed a predictive model for residual stress in orthogonal cutting considering the effect of shear plane and the edge hone, in which the hybrid algorithm [8] is adopted. Similarly, Lazoglu et al. [9] presented an enhanced analytical model for residual stress prediction in orthogonal machining with the algorithm proposed in [10], considering the superposition of thermal and mechanical stresses.

The physical based residual stress prediction for milling process is seldom reported in the literature for its complicacy. Recently, Su et al. [11] developed an analytical model for the residual stresses in milling, which incorporated the prediction of cutting force and temperature. The model performed well in predicting the trends of residual stresses for various milling conditions, although an assumption of largest depth of cut (DOC) during mechanic loading was made in the model, which led to overestimated forces at the surface.

In order to improve the accuracy of the analytical model for the residual stress prediction in flank milling, we propose a new analytical model of residual stress, in which the sequential variable loading in flank milling is taken into consideration for the first time. An incremental elasto-plastic method followed by a relaxation procedure is used to get the stress-strain history of an arbitrary point in the subsurface so as to predict the residual stress retained in the workpiece after several loading cycles.

2. Analytical model of residual stress in 2D orthogonal flank milling

According to the definition of flank milling [1], chips are formed along the flank side of the tool, as is shown in Fig. 1. For flank milling in the shop floor, the spiral end mill is generally used so as to make the variation of cutting force smooth. Owing to the helical angle, three dimensional oblique cutting is involved, which complicates the analysis of the contact stress beneath the machined surface. In this paper, 2D orthogonal flank milling is considered for simplification so that it turned to be a plane strain problem and the cutting force can be treated as a line load. It should be noted that the simplified model still keeps the main feature of loading in flank milling and can be applied to the end mill with a small helical angle.

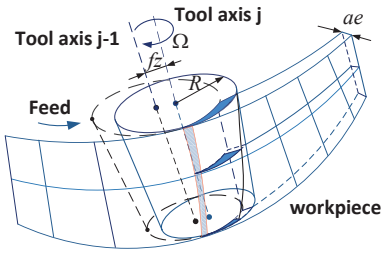

Fig. 1. Geometry of general flank milling with a spiral end mill

It has been a consensus that the mechanical impact in machining process is prone to introduce compressive residual stress while thermal impact is prone to cause tensile residual stress. When it comes to milling titanium alloys, however, most experimental results in literature show that the residual stress is compressive in nature [2, 3] and the mechanical load dominates the residual stress formation especially at low cutting speed [11-13]. This can be attributed to the low thermal expansion coefficient of titanium alloy, which keeps the thermal stress at a relatively low level within a thin thermo-affected layer. Hence, the model can be further simplified if the thermal effects can be ignored.

In summary, the essential simplifications in the model include:

- 2D orthogonal flank milling
- The thermal effects are ignored

2.1. Mechanic load of 2D orthogonal flank milling

Fig. 2 illustrates the definition of coordinate systems and the cutting force applied to the machined surface in 2D orthogonal milling.

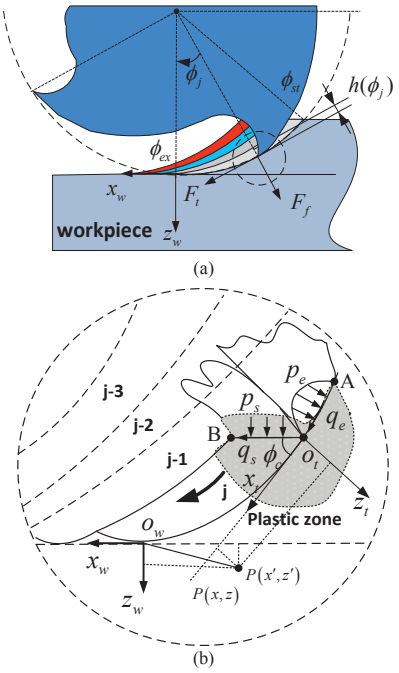

Fig. 2. (a) Global geometry of 2D orthogonal flank milling; (b) loading of shear plane and flank wear land at the newly formed surface.

The mechanistic model is adopted and the cutting forces include both the shearing forces F_{tc}, F_{fc} in the primary shear zone and the edge forces F_{te}, F_{fe} in the tertiary deformation zone:

$$\begin{aligned} F_t &= F_{tc} + F_{te} \\ F_f &= F_{fc} + F_{fe} \end{aligned} \tag{1}$$

The shearing forces are in proportion to the uncut chip thickness h, while the edge forces are determined by the axial depth b:

$$\begin{aligned} F_t &= K_{tc} bh + K_{te} b \\ F_f &= K_{fc} bh + K_{fe} b \end{aligned} \tag{2}$$

The uncut chip thickness of the *j*th tooth varies periodically with the immersion angle ϕ_j :

$$h(\phi_j) = g(\phi_j) f_z \sin\phi_j \tag{3}$$

$$g(\phi_j) = \begin{cases} 1 & \text{if } \phi_j \in [\phi_{st}, \phi_{ex}] \\ 0 & \text{otherwise} \end{cases} \tag{4}$$

where f_z denotes feed per tooth, $g(\phi_j)$ is the switch function and ϕ_{st}, ϕ_{ex} are the entrance angle and exit angle respectively.

The cutting coefficients K_{tc}, K_{fc} and edge coefficients K_{te}, K_{fe} can be calibrated using quick mechanistic approach proposed by Budak and Altintas [14]. The cutting coefficients K_{tc}, K_{fc} can be expressed as follows:

$$K_{tc} = \tau_s \frac{\cos(\beta_\alpha - \alpha_r)}{\sin\phi_c \cos(\phi_c + \beta_\alpha - \alpha_r)}$$
$$K_{fc} = \tau_s \frac{\sin(\beta_\alpha - \alpha_r)}{\sin\phi_c \cos(\phi_c + \beta_\alpha - \alpha_r)} \tag{5}$$

The shear stress τ_s , shear angle ϕ_c , friction angle β_a and rake angle α_r can be calculated from the cutting force components and cutting ratio, using the orthogonal cutting theory [15].

2.2. Periodically varying distributed loading

As for residual stress modeling in orthogonal turning, Su and Liang [7] have taken into account both the shearing and the ploughing effects. It is the varying immersion angle that makes the difference in milling.

As is shown in Fig. 2, the mechanic loading applied to the machined surface is similar to the distributed loading in cyclic rolling contact. In rolling contact, one loading cycle is defined as the movement of an arbitrary point beneath the fixed contact region from $x = +\infty$ to $x = -\infty$. In 2D orthogonal flank milling, however, the contact region is movable following the cutting edge with trochoid trajectory. Here, we define one cycle as the movement of a cutting edge while $\phi \in [\phi_{st}, \phi_{ex}]$. It is obvious that the loading histories of the points beneath every scallop generated in milling are the same. Hence, the variation of residual stress is periodic in the feeding direction in nature.

For an arbitrary point $P(x, y)$ in the workpiece coordinates $\{x_w o_w y_w\}$, mechanic stresses due to shearing and ploughing effects can be expressed concisely in the tool coordinates $\{x_t o_t y_t\}$ fixed with the cutting edge, as is demonstrated by Jacobus [16, 17] and Su [11]. After coordinate transformation, the point $P(x, y)$ becomes $P(x', y')$ in $\{x_t o_t y_t\}$:

$$\begin{bmatrix} x' \\ z' \end{bmatrix} = \begin{bmatrix} \cos\phi_j & \sin\phi_j \\ -\sin\phi_j & \cos\phi_j \end{bmatrix} \begin{bmatrix} x \\ z \end{bmatrix} + \begin{bmatrix} r\sin\phi_j \\ r(1-\cos\phi_j) \end{bmatrix} \tag{6}$$

Now, the problem can be treated in the same way as rolling contact. In the semi-infinite plane, the analytical expressions of stress field due to distributed normal pressure $p(s)$ and tangential tractions $q(s)$ are [18]:

$$\sigma_{xx} = -\frac{2z}{\pi}\int_{-a}^{a} \frac{p(s)(x-s)^2}{\left((x-s)^2+z^2\right)^2} ds - \frac{2}{\pi}\int_{-a}^{a} \frac{q(s)(x-s)^3}{\left((x-s)^2+z^2\right)^2} ds$$
$$\sigma_{zz} = -\frac{2z^3}{\pi}\int_{-a}^{a} \frac{p(s)}{\left((x-s)^2+z^2\right)^2} ds - \frac{2z^2}{\pi}\int_{-a}^{a} \frac{q(s)(x-s)}{\left((x-s)^2+z^2\right)^2} ds \tag{7}$$
$$\tau_{xz} = -\frac{2z^2}{\pi}\int_{-a}^{a} \frac{p(s)(x-s)}{\left((x-s)^2+z^2\right)^2} ds - \frac{2z}{\pi}\int_{-a}^{a} \frac{q(s)(x-s)^2}{\left((x-s)^2+z^2\right)^2} ds$$

where *a* denotes the half-width of the loading area. As for the case on the shearing plane, a varies with the immersion angle and shear angle:

$$a = \frac{O_t B}{2} = \frac{f_z \sin\phi_j}{2\sin\phi_c} \tag{8}$$

In this paper, the influence of chip thickness on the shear angel ϕ_c is ignored. Thus the shear angle is treated as a constant for simplification.

Both the normal pressure P_s and tangential traction q_s on the shear plane are assumed to be uniformly distributed, which has been adopted in previous research [11, 13]. According to Merchants' hodograph of cutting force, we have:

$$p_s = \tau_s \tan(\phi_c + \beta_\alpha - \alpha_r) \tag{9}$$

$$q_s = \tau_s \tag{10}$$

In the tertiary deformation zone, the ploughing force model proposed by Waldorf [19] is adopted. The forces caused by the flank wear land of worn tool are not considered here. According to the slip-line model of ploughing, both the normal pressure and the shear stress on the plough area are uniformly distributed and expressed as:

$$p_e = \begin{bmatrix} \left(1+2\theta+2\gamma+\sin(2\eta_p)\right)\sin(\phi_c-\gamma+\eta_p)+ \\ \cos(2\eta_p)\cos(\phi_c-\gamma+\eta_p) \end{bmatrix} \tau_s$$
$$q_e = \begin{bmatrix} \left(1+2\theta+2\gamma+\sin(2\eta_p)\right)\cos(\phi_c-\gamma+\eta_p)- \\ \cos(2\eta_p)\sin(\phi_c-\gamma+\eta_p) \end{bmatrix} \tau_s \tag{11}$$

$$K_{te} = p_e \cdot CA$$
$$K_{fe} = q_e \cdot CA \tag{12}$$

where θ , γ and η_p are slip-line angles and *CA* is the length of ploughing area in the slip-line field. The details can be referenced to [19].

Since the stress fields expressed in Eq. (7) are defined in local coordinates, transformations are required so as to superpose all the stress components in $\{x_t o_t y_t\}$ [20]. A brief description is provided as follows:

$$[\sigma'_{shear}] = [Q][\sigma^*_{shear}][Q]^T \tag{13}$$

$$[Q] = \begin{bmatrix} \cos\phi_c & \sin\phi_c \\ -\sin\phi_c & \cos\phi_c \end{bmatrix} \tag{14}$$

$$[\sigma'_{ij}] = [\sigma'_{shear}] + [\sigma'_{edge}] \tag{15}$$

where $[\sigma^*_{shear}]$ denote the stresses due to shear plane in its local coordinates. $[Q]$ is the rotation matrix from the local coordinates of the inclined shear plane to $\{x_t o_t y_t\}$. $[\sigma'_{shear}]$

and $\left[\sigma'_{edge}\right]$ are the stresses due to the shear plane and the tertiary deformation zone respectively. $\left[\sigma'_{ij}\right]$ are the total stresses in $\{x_t o_t y_t\}$.

For every step of the rotating tool in contact with the workpiece, the stresses $\left[\sigma_{ij}\right]$ at $P(x,y)$ can be expressed as:

$$\left[\sigma_{ij}\right]=[R]\left[\sigma'_{ij}\right][R]^T \tag{16}$$

$$[R]=\begin{bmatrix}\cos\phi_j & \sin\phi_j\\ -\sin\phi_j & \cos\phi_j\end{bmatrix} \tag{17}$$

where $[R]$ is the rotation matrix from $\{x_t o_t y_t\}$ to $\{x_w o_w y_w\}$.

2.3. Residual stress modeling

With elastic stress field calculated, the residual stress of flank milled surface can be calculated using the analytical approaches developed for elastic-plastic two-dimensional rolling/sliding contact [10, 21, 22]. In this paper, the hybrid algorithm developed by McDowell [8] is adopted, which enables the prediction of subsurface cyclic plasticity and residual stress for loading conditions with wide range. Here, a brief description of the hybrid algorithm is provided.

A blending function ψ which is dependent on the instantaneous value of the modulus ratio h/G is introduced:

$$\psi=1-\exp\left(-\kappa\frac{3}{2}\frac{h}{G}\right) \tag{18}$$

where G is the elastic shear modulus, h is the modulus function and κ is an algorithm constant which affects the nature of the blending greatly.

The von Mises yield surface is defined by:

$$F=\frac{1}{2}\left(s_{ij}-\alpha_{ij}\right)\left(s_{ij}-\alpha_{ij}\right)-k^2=0 \tag{19}$$

where k is the shear yield stress and s_{ij} are the components of the deviatoric stress. α_{ij} are the components of the deviatoric backstress. The linear kinematic hardening rule is used:

$$\dot{\alpha}_{ij}=\left\langle \dot{s}_{kl}n_{kl}\right\rangle n_{ij} \tag{20}$$

where n_{ij} represent the components of the unit normal in the direction of the plastic strain rate $\dot{\varepsilon}^p_{ij}$ on the yield surface:

$$\dot{\varepsilon}^p_{ij}=\frac{1}{h}\left\langle \dot{s}_{kl}n_{kl}\right\rangle n_{ij} \tag{21}$$

$$n_{ij}=\frac{s_{ij}-\alpha_{ij}}{\sqrt{2}k} \tag{22}$$

Incremental form is adopted for the elastic-plastic loading. The elastic stress field introduced by the varying load is enforced:

$$\dot{\sigma}_{xx}=\dot{\sigma}^{el}_{xx},\ \dot{\sigma}_{zz}=\dot{\sigma}^{el}_{zz},\ \dot{\tau}_{xz}=\dot{\tau}^{el}_{xz} \tag{23}$$

where $\dot{\sigma}^{el}_{xx}$, $\dot{\sigma}^{el}_{zz}$ and $\dot{\tau}^{el}_{xz}$ are elastic solutions.

The plane strain condition is involved:

$$\dot{\varepsilon}_{yy}=0 \tag{24}$$

$$\dot{\sigma}_{yy}=\nu\left(\dot{\sigma}^{el}_{xx}+\dot{\sigma}^{el}_{zz}\right) \tag{25}$$

For elastic-plastic loading, the blending function ψ is used to impose the x-direction strain rate according to:

$$\begin{aligned}\dot{\varepsilon}_{xx}&=\frac{\dot{\sigma}_{xx}}{E}-\frac{\nu}{E}(\dot{\sigma}_{yy}+\dot{\sigma}^{el}_{zz})+\frac{1}{h}(\dot{\sigma}_{xx}n_{xx}+\dot{\sigma}_{yy}n_{yy}+\dot{\sigma}^{el}_{zz}n_{zz}+2\dot{\tau}^{el}_{xz}n_{xz})n_{xx}\\&=\psi[\frac{\dot{\sigma}^{el}_{xx}}{E}-\frac{\nu}{E}(\dot{\sigma}_{yy}+\dot{\sigma}^{el}_{zz})+\frac{1}{h}(\dot{\sigma}^{el}_{xx}n_{xx}+\dot{\sigma}_{yy}n_{yy}+\dot{\sigma}^{el}_{zz}n_{zz}+2\dot{\tau}^{el}_{xz}n_{xz})]n_{xx}\end{aligned} \tag{26}$$

The plane strain condition in the y-direction gives:

$$\dot{\varepsilon}_{yy}=\frac{\dot{\sigma}_{xx}}{E}-\frac{\nu}{E}(\dot{\sigma}_{xx}+\dot{\sigma}^{el}_{zz})+\frac{1}{h}(\dot{\sigma}_{xx}n_{xx}+\dot{\sigma}_{yy}n_{yy}+\dot{\sigma}^{el}_{zz}n_{zz}+2\dot{\tau}^{el}_{xz}n_{xz})n_{yy}=0 \tag{27}$$

Eqs. (26) and (27) are solved simultaneously to get the stress increments $\dot{\sigma}_{xx}$ and $\dot{\sigma}_{yy}$.

At the end of each loading cycle, a relaxation procedure is needed to incrementally relax the none-zero components according to the boundary condition for residual stress [21]:

$$\sigma^R_{zz}=0,\ \tau^R_{xz}=0,\ \varepsilon^R_{xx}=0 \tag{28}$$

After relaxation, the residual stresses σ^r_{xx} and σ^r_{yy} caused by the current cycle are achieved, which are used as initial condition in the next loading cycle. Hence, several loading cycles are needed for numerical integration in the simulation of residual stress in milling.

3. Simulations and discussion

Flank milling of Ti-6Al-4V are conducted using carbide cutter JHP770 provided by SECO™, which has four flutes, diameter D=10mm, edge radius r_e=25μm, rake angle α_r=6° and helical angel β=42°. The cutting conditions are shown in Table 1.

Table 1. Cutting conditions for flank milling

case	Speed (m/min)	Feed rate (mm/tooth)	Radial DOC (mm)	Axial DOC (mm)	Type
1	50	0.06	0.2	10	Down
2	50	0.06	0.5	6	Down
3	50	0.12	0.2	10	Down
4	50	0.12	0.5	6	Down

To utilize the proposed analytical model, the effect of helical angle is ignored and the problem is considered to be two-dimensional. The orthogonal cutting database of Ti6Al4V is employed [14], which gives the shear stress $\tau_s=613$MPa, the friction angle $\beta_a=20.8°$, the mean shear angle $\phi_c=25°$. The length of ploughing area CA=0.028mm.

The normal pressure and tangential stress on the shear plane are $p_s=0.83\tau_s$ and $q_s=\tau_s$, thus the average cutting coefficients are $K_{tc}=1813\text{N/mm}^2$ and $K_{fc}=480\text{N/mm}^2$. The normal pressure and tangential stress on the plough area are $p_e=2.65\tau_s$ and $q_e=1.01\tau_s$, thus the edge force coefficients are $K_{te}=17\text{N/mm}$ and $K_{fe}=45\text{N/mm}$.

Without loss of generality, we take an arbitrary point beneath the bottom of the scallop as an example in the following sections. The variations of stress component σ_{xx} and the second invariant J_2 are shown in Fig. 3 and Fig. 4. It is

noted that, the stresses are identical for the cases with the same feed per tooth at any immersion angle as long as the cutting edge is in contact with the workpiece. Hence, the stress variation for case 1 and case 2 are the same. The same goes for case 3 and case 4.

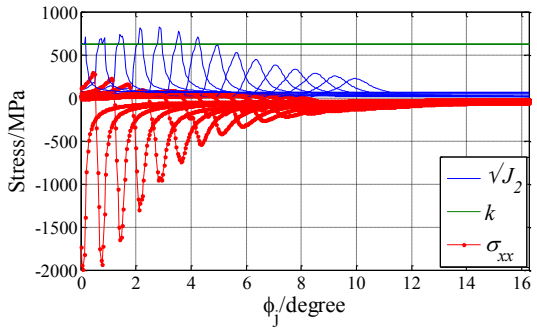

Fig. 3. Stress variation for cases 1 and 2.

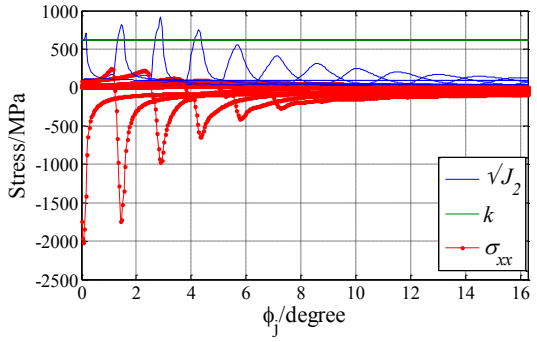

Fig. 4. Stress variation for cases 3 and 4.

In the finish process, the stress is elastic in most of loading cycles, which has no impact on the generation of residual stress. Only the last cycles with small immersion angles cause plastic deformation. As a result, the radial DOC has almost no influence on the residual stress, when it exceeds a critical value. Additionally, the simulation results demonstrate that feed rate influence the number of effective loading cycles. In contrast to cases 3 and 4, the small feed rate in cases 1 and 2 increases the effective loading cycle dramatically.

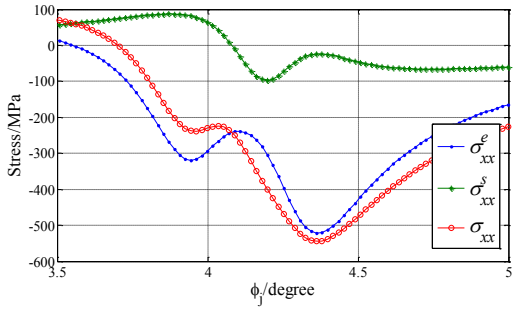

Fig. 5. Comparison between the stress components due to cutting edge, shearing plane and the total stress.

When the immersion angle approaches zero, stress introduced by the shearing plane is small and the main mechanic load comes from the plough effect of cutting edge, as is shown in Fig. 5. As a result, it is the ploughing forces that dominate the generation of residual stress in flank milling. Similar conclusion is reported in references [23-25].

The residual stress and back stress produced in the previous loading cycles will influence the current one. In our cases, the simulation result demonstrates that the residual stresses reach steady states after a few effective cycles.

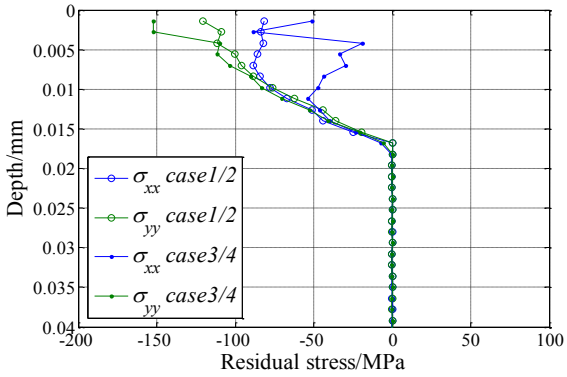

Fig. 6. Prediction of Residual stresses

The predictions for the steady residual stresses after flank milling are shown in Fig. 6. As has been discussed previously, the radial DOC almost has no influence on the results in these cases. What is more, the residual stress in the axial direction is more compressive than the residual stress in the feed direction. The depth of compressive layer approximates the radius of the cutting edge.

X-ray diffraction is utilized to measure the residual stress. The radiation is Copper Kα, with a Bragg angle of 142 degrees for the crystallographic plane <213>. Four tilt angles are employed using the $\sin^2\psi$ method. A scanning step of 0.1 degrees is adopted for angle θ ranging from 137~147 degrees, with the exposure time for each step set as 2 seconds. Limited by experiment condition, only the residual stresses on the surface are measured and the residual stress profiles along the depth are not achieved.

	feed	axial
case1	-320	-190
case2	-153.3	-303.4
case3	-238.9	-230
case4	-245.2	-303.1

Fig. 7. Residual stresses measured in experiment.

The experiment results are illustrated in Fig. 7. All the residual stresses on the surface are compressive after flank milling of Ti-6Al-4V. The residual stresses are close to each other in case 3 and case 4, just as the prediction shows. In addition, residual stress in axial direction is a little more compressive than the residual stress in feed direction, which are validated in case 2 and case 4. The discrepancy between the prediction and experimental result can be attributed to the helical angle and run-out of the cutter, which will change the actual uncut chip thickness and the mechanic loading condition. Moreover, the plastic constitutive parameters and non-linear kinematic hardening of material affects the magnitude of the residual stress considerably.

In spite of this, the model provides an efficient framework to consider the variable loading cycles for the prediction of residual stress in flank milling and predicts the trend of residual stresses with various cutting conditions. Comprehensive cutting force model can be employed in this framework so as to consider the influence of run-out and variable pitch on the residual stress in flank milling.

4. Conclusion

An analytical model is proposed for the prediction of residual stress in flank milling of Ti-6Al-4V. An effective framework considering the cyclic varying load in 2D orthogonal flank milling is presented. In addition to high computation efficiency, the model reveals the main difference between milling and turning in the formation of residual stress.

It is found that the residual stress in flank milling is mainly attributed to the plough effect of cutting edge in a few loading cycles. While the feed rate influences the effective cycle times, the radial depth of cut has almost no influence on the residual stress when it exceeds a critical value. The simulation indicates that the flank milled surface shows more compressive residual stress in the axial direction than in the feed direction. The model is verified by milling tests, in which X-ray diffraction is employed for the measurement of residual stress on the surface.

Acknowledgements

This work was partially supported by the National Natural Science Foundation of China (51375005) and the National Basic Research Program of China (2014CB046704).

References

[1] Harik, R.F., Gong, H., Bernard, A., 2013, 5-axis flank milling: A state-of-the-art review, Computer-Aided Design, 45/3:796-808.

[2] Ulutan, D., Ozel, T., 2011, Machining induced surface integrity in titanium and nickel alloys: A review, International Journal of Machine Tools and Manufacture, 51/3:250-280.

[3] Guo, Y.B., Li, W., Jawahir, I.S., 2009, Surface integrity characterization and prediction in machining of hardened and difficult-to-machine alloys: A state-of-art research review and analysis, Machining Science and Technology, 13/4:437-470.

[4] Liu, C.R., Barash, M.M., 1976, The Mechanical State of the Sublayer of a Surface Generated by Chip-Removal Process—Part 1: Cutting With a Sharp Tool, Journal of Manufacturing Science and Engineering, 98/4:1192-1199.

[5] Liu, C.R., Barash, M.M., 1976, The Mechanical State of the Sublayer of a Surface Generated by Chip-Removal Process—Part 2: Cutting With a Tool With Flank Wear, Journal of Manufacturing Science and Engineering, 98/4:1202-1208.

[6] Jacobus, K., DeVor, R.E., Kapoor, S.G., 2000, Machining-induced residual stress: Experimentation and modeling, Journal of Manufacturing Science and Engineering, 122/1:20-31.

[7] Liang, S.Y., Su, J.C., 2007, Residual Stress Modeling in Orthogonal Machining, CIRP Annals - Manufacturing Technology, 56/1:65-68.

[8] McDowell, D.L., 1997, An approximate algorithm for elastic-plastic two-dimensional rolling/sliding contact, Wear, 211/2:237-246.

[9] Lazoglu, I., Ulutan, D., Alaca, B.E., Engin, S., Kaftanoglu, B., 2008, An enhanced analytical model for residual stress prediction in machining, CIRP Annals - Manufacturing Technology, 57/1:81-84.

[10] Jiang, Y., Sehitoglu, H., 1994, An Analytical Approach to Elastic-Plastic Stress Analysis of Rolling Contact, Journal of Tribology, 116/3:577-587.

[11] Su, J., Young, K.A., Ma, K., Srivatsa, S., Morehouse, J.B., Liang, S.Y., 2013, Modeling of residual stresses in milling, The International Journal of Advanced Manufacturing Technology, 65/5-8:717-733.

[12] Lin, Z., Lee, B., 1995, An investigation of the residual stress of a machined workpiece considering tool flank wear, Journal of Materials Processing Technology, 51/1-4:1-24.

[13] Lin, Z., Lin, Y., Liu, C.R., 1991, Effect of thermal load and mechanical load on the residual stress of a machined workpiece, International Journal of Mechanical Sciences, 33/4:263-278.

[14] Budak, E., Armarego, E.J.A., Altintaş, Y., 1996, Prediction of milling force coefficients from orthogonal cutting data, Journal of Manufacturing Science and Engineering, 118 /2:216-224.

[15] Altintas, Y., 2012, Manufacturing Automation: Metal Cutting Mechanics, Machine Tool Vibrations, and CNC Design, Cambridge University Press, Combridge.

[16] Jacobus, K., DeVor, R.E., Kapoor, S.G., Peascoe, R.A., 2001, Predictive model for the full biaxial surface and subsurface residual stress profiles from turning, Journal of Manufacturing Science and Engineering, 123/4:537-546.

[17] Jacobus, K., Kapoor, S.G., DeVor, R.E., 2001, Experimentation on the residual stresses generated by endmilling, Journal of Manufacturing Science and Engineering, 123/4:748-753.

[18] Johnson, K.L., 1987, Contact Mechanics, Combridge Unisversity Press, Combridge.

[19] Waldorf, D.J., DeVor, R.E., Kapoor, S.G., 1998, A slip-line field for ploughing during orthogonal cutting, Journal of Manufacturing Science and Engineering, 120/4:693-699.

[20] Su, J.C., 2006, Residual stress modeling in machining processes. Ph.D., Georgia Institute of Technology, Atlanta.

[21] Merwin, J.E., Johnson, K.L., 1963, An Analysis of Plastic Deformation in Rolling Contact, Proceedings of the Institution of Mechanical Engineers, 177/25:676-690

[22] McDowell, D.L., Moyar, G.J., 1991, Effects of non-linear kinematic hardening on plastic deformation and residual stresses in rolling line contact, Wear, 144/1-2:19-37

[23] Denkena, B., Nespor, D., Böß, V., Köhler, J., 2014, Residual stresses formation after re-contouring of welded Ti-6Al-4V parts by means of 5-axis ball nose end milling, CIRP Journal of Manufacturing Science and Technology, 7/4:347-360.

[24] Denkena, B., Koehler, J., Rehe, M., 2012, Influence of the Honed Cutting Edge on Tool Wear and Surface Integrity in Slot Milling of 42CrMo4 Steel, Procedia CIRP, 1:190-195.

[25] Schulze, V., Autenrieth, H., Deuchert, M., Weule, H., 2010, Investigation of surface near residual stress states after micro-cutting by finite element simulation, CIRP Annals - Manufacturing Technology, 59/1:117-120